

# Variations of the stellar initial mass function in semi-analytical models: implications for the mass assembly and the chemical enrichment of galaxies in the GAEA model.

Fabio Fontanot<sup>1\*</sup>, Gabriella De Lucia<sup>1</sup>, Michaela Hirschmann<sup>2</sup>, Gustavo Bruzual<sup>3</sup>, Stéphane Charlot<sup>2</sup> and Stefano Zibetti<sup>4</sup>

<sup>1</sup> INAF - Astronomical Observatory of Trieste, via G.B. Tiepolo 11, I-34143 Trieste, Italy

<sup>2</sup> UPMC-CNRS, UMR7095, Institut d'Astrophysique de Paris, 75014, Paris, France

<sup>3</sup> Instituto de Radioastronomía y Astrofísica, UNAM, Campus Morelia, C.P. 58089, Morelia, México

<sup>4</sup> INAF-Osservatorio Astrofisico di Arcetri, Largo Enrico Fermi 5, I-50125 Firenze, Italy

Accepted ... Received ...

## ABSTRACT

In this work, we investigate the implications of the Integrated Galaxy-wide stellar Initial Mass Function (IGIMF) approach in the framework of the semi-analytic model GAEA (GALaxy Evolution and Assembly), which features a detailed treatment of chemical enrichment and stellar feedback. The IGIMF provides an analytic description of the dependence of the stellar IMF shape on the rate of star formation in galaxies. We find that our model with a universal IMF predicts a rather flat  $[\alpha/\text{Fe}]$ -stellar mass relation. The model assuming the IGIMF, instead, is able to reproduce the observed increase of  $\alpha$ -enhancement with stellar mass, in agreement with previous studies. This is mainly due to the fact that massive galaxies are characterized by larger star formation rates at high-redshift, leading to stronger  $\alpha$ -enhancement with respect to low-mass galaxies. At the same time, the IGIMF hypothesis does not affect significantly the trend for shorter star formation timescales for more massive galaxies. We argue that in the IGIMF scenario the  $[\alpha/\text{Fe}]$  ratios are good tracers of the highest star formation events. The final stellar masses and mass-to-light-ratio of our model massive galaxies are larger than those estimated from the synthetic photometry assuming a universal IMF, providing a self-consistent interpretation of similar recent results, based on dynamical analysis of local early type galaxies.

**Key words:** galaxies: formation - galaxies: evolution - galaxies: abundances - galaxies: fundamental parameters - galaxies: stellar content

## 1 INTRODUCTION

Among the different facets characterising the process of star formation in galaxies, the shape of the stellar initial mass function (IMF, defined as the number of stars formed per stellar mass bin in a given star formation episode) represents an aspect which has not been fully constrained yet. From a theoretical perspective, a key problem is the lack of a detailed understanding of the chain of events leading to the collapse and fragmentation of unstable molecular clouds (Krumholz 2014). On the observational side, direct measurements of the IMF via stellar counts are possible only in the solar neighbourhood and/or in the closest galactic systems (i.e. the Milky Way and its largest satellites). Despite some relevant uncertainties both at the low-mass-end (in the brown dwarfs regime) and at the high-

mass end (i.e. the exact location of the cutoff), the shape of the observed IMF shows a remarkable invariance in most Galactic environments (with the relevant exception of the densest regions of the Galactic centre, Klessen et al. 2007). Several functional representations of the IMF have been proposed in the literature, from early suggestions of a single power-law (Salpeter 1955) to a more recent broken power-law (Kroupa 2001) and lognormal with a power-law tail (Chabrier 2003).

The notion of a *universal IMF* has been challenged theoretically by a number of models exploring the expected impact of small scale physical properties of the inter-stellar medium (ISM) on the star formation process (Weidner & Kroupa 2005; Klessen et al. 2005; Hennebelle & Chabrier 2008; Hopkins 2012; Papadopoulos 2010; Papadopoulos et al. 2011; Narayanan & Davé 2013, among others). These models predict a range of possible shapes for the IMF as a function of the physical properties of

\* E-mail: fontanot@oats.inaf.it

star forming regions, but a direct testing of the range of possible conditions (i.e. beyond the Local Group environment) is currently impossible, as we have access only to the integrated light and not to the resolved stellar populations in distant galaxies. Several indirect observational evidences for a varying IMF have, however, been reported in the literature, both in late-type galaxies (Hoversten & Glazebrook 2008; Gunawardhana et al. 2011) and in early type samples (Cappellari et al. 2012; Conroy & van Dokkum 2012; Ferreras et al. 2013), as well as in dwarf galaxies (McWilliam et al. 2013). These claims have raised considerable debate on the interpretation of the data, and on the overall consistency between these results (see e.g. Smith 2014). It is thus timely to test the hypothesis of a varying IMF in a cosmological context, in order to identify the constraints coming from the photometric, dynamical and physical properties of galaxy populations and to correctly interpret the wealth of data currently available. A variable IMF would indeed impact the galaxy properties in many aspects, ranging from the chemical enrichment patterns to the efficiency of stellar feedback, with critical implications on the fraction of baryonic mass locked in long lived stars.

Chemical abundance patterns have been used for a long time as an indication of the star formation timescale of integrated stellar populations. Indeed, the abundance ratio between  $\alpha$  elements (O, Mg, Si) and iron is critically sensitive to the relative abundance between short-lived type II core-collapse supernovae (SN, whose main ejecta are  $\alpha$  elements) and long-lived Type Ia SN (the main iron-peak producers), whose progenitors have lifetimes of the order of Gyrs (see e.g. Pipino & Matteucci 2004, and references herein). Assuming a universal IMF, higher levels of  $\alpha$ -enhancement require shorter star formation timescales, so that most of the stars in the system form before the ISM is iron-enriched by SNIa. The observed increase of  $[\alpha/\text{Fe}]$  ratio with stellar mass in local early-type galaxies is thus interpreted as an indication for shorter star formation timescales for massive galaxies, with respect to their low-mass counterparts (Matteucci 1994). This has been considered a long-standing problem for theoretical models of galaxy formation and evolution (see e.g. Thomas et al. 2005). In Fontanot et al. (2009) we analysed the different definitions of “downsizing” trends but could not address explicitly the abundance ratio trends as a function of stellar mass, which we dubbed *chemoarcheological downsizing*.

Several groups have proposed solutions to this puzzle in the context of the concordance cosmological model, using both hydrodynamical simulations and semi-analytical models (SAMs). Two main approaches have been proposed, mainly focusing on an increased role of feedback and/or variations of the IMF. Pipino et al. (2009) and Calura & Menci (2011) claim that an increased role of AGN feedback (in the latter model associated with strong stellar feedback in starburst induced in galaxy interactions) is able to regulate star formation timescales in the progenitors of massive galaxies. We note that in the latter model chemical enrichment is computed post-processing star formation histories extracted from the SAM. Similar results have been obtained in the framework of hydrodynamical simulations (Segers et al. 2016). Variations of the IMF have also been suggested as possible drivers of the observed trends. For example, Nagashima et al. (2005) showed that models assuming a Top-Heavy IMF in starbursts associated with galaxy mergers are in better agreement with the  $[\alpha/\text{Fe}]$  ratios observed for local elliptical galaxies, than models using a universal IMF. The first attempt to include a theoretically based model for a varying IMF in a theoretical model of galaxy evolution has been presented in Gargiulo et al. (2015, G15 hereafter). They implemented

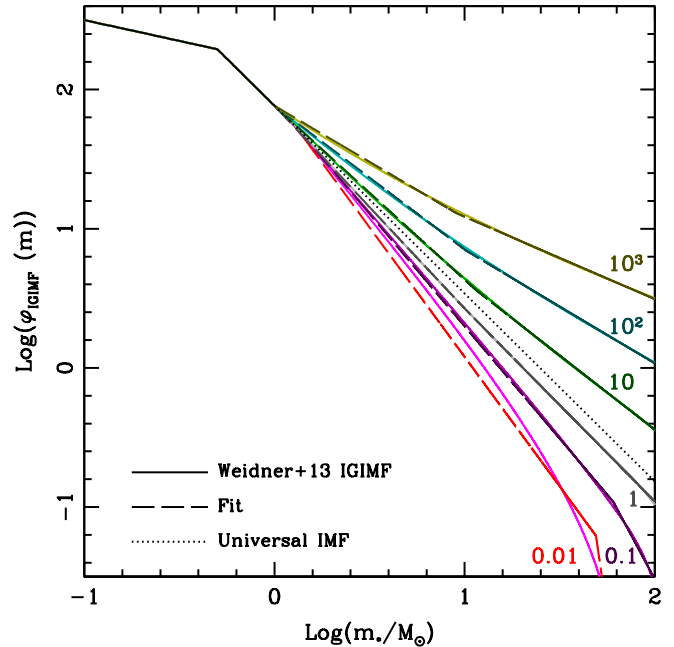


**Figure 1.** Integrated galaxy-wide IMF for different star formation rates. Each IGIMF is normalised to the same  $m_* < 1 M_\odot$  values. Solid lines correspond to the results of the explicit integration using Eq. 1 to 7. Dashed lines refer to the four-slopes fits used in our models (see text for more details). The universal IMF by Kroupa (2001) is shown as a dotted line.

the integrated galaxy-wide IMF (IGIMF) model, first proposed by Weidner & Kroupa (2005), in the Semi-Analytical Galaxies (SAG) model (Cora 2006). SAG features a chemical enrichment scheme which tracks the evolution of individual chemical elements, taking into account the different timescales associated with different sources (i.e. SNIa, SNII, stellar winds). In particular, G15 consider the IGIMF formulation proposed by Weidner et al. (2011), which relates the shape of the IMF to the star formation rate (SFR). Their results show that by using a varying IMF it is possible to recover the positive trend of  $[\alpha/\text{Fe}]$  ratio with stellar mass, but they did not analyse the implications of this assumption on the overall assembly and star formation evolution of model galaxies. Finally, an earlier attempt to compare the predictions of both theoretically and observationally based IMF variation models in the SAM framework has been presented in Fontanot (2014).

In this paper, we follow an approach similar to G15. Among the theoretical models predicting IMF variations tested in Fontanot (2014), we choose, like G15, to focus on the IGIMF model, which combines a limited number of physically motivated assumptions in a set of differential equations, to predict the IMF shape as a function of the physical properties of the star forming regions. It is possible to reformulate the key equations as a function of the (galaxy-wide) SFR, thus providing an elegant formalism, well suited to be included in a SAM. We thus interface the most recent formulation of the IGIMF model by Weidner et al. (2013) in the Galaxy Evolution and Assembly (GAEA) model (De Lucia et al. 2014; Hirschmann et al. 2015). As SAG, GAEA implements a sophisticated model for chemical enrichment, taking into account the finite lifetimes (and differential yields) of stars of different mass. On top of that, GAEA also features an updated formulation for stellar feedback, inspired by numerical simulations, which allows us to

correctly reproduce the redshift evolution of the galaxy stellar mass function.

This paper is organised as follows. In Section 2 we will outline the basis for the IGIMF theory as presented in Weidner et al. (2013). We will then describe its semi-analytic implementation in Section 3. We will present and discuss our results in Section 4. Finally, we will summarise our conclusions in Section 5.

## 2 INTEGRATED GALAXY-WIDE IMF THEORY

We compute the integrated galaxy-wide IMF (IGIMF) associated with a given SFR following the work of Weidner & Kroupa (2005, see also Kroupa et al. 2013 for a review).

Stars form in the densest regions of molecular clouds (MC). The IMF associated with individual stellar clusters is universal and can be well represented by a broken power law (Kroupa 2001):

$$\varphi_*(m) = \begin{cases} \left(\frac{m}{m_{\text{low}}}\right)^{-\alpha_1} & m_{\text{low}} \leq m < m_0 \\ \left(\frac{m}{m_0}\right)^{-\alpha_1} \left(\frac{m}{m_0}\right)^{-\alpha_2} & m_0 \leq m < m_1 \\ \left(\frac{m}{m_0}\right)^{-\alpha_1} \left(\frac{m_1}{m_0}\right)^{-\alpha_2} \left(\frac{m}{m_1}\right)^{-\alpha_3} & m_1 \leq m \leq m_{\text{max}} \end{cases} \quad (1)$$

where  $m_{\text{low}} = 0.1$ ,  $m_0 = 0.5$ ,  $m_1 = 1.0$ ,  $\alpha_1 = 1.3$ ,  $\alpha_2 = \alpha_3 = 2.35$ . The shape of the IMF of individual clouds is usually calibrated on local observations, but it agrees well with theoretical calculation based on the fragmentation of giant molecular clouds (see e.g. Hennebelle & Chabrier 2008, and reference herein).

The key assumption of the IGIMF approach is that the global star formation activity of the galaxy is well described as the sum over individual MCs, whose mass function is assumed to be a power-law

$$\varphi_{\text{CL}}(M_{\text{cl}}) \propto M_{\text{cl}}^{-\beta}, \quad (2)$$

with local surveys of young embedded clusters suggesting  $\beta = 2$  (Lada & Lada 2003). The maximum value of the mass of a star cluster  $M_{\text{cl}}^{\text{max}}$  to form as a function of the instantaneous SFR has been derived in Weidner et al. (2004) using observed maximum star cluster masses (but it can be derived analytically from optimal sampling arguments Kroupa et al. 2013):

$$\log M_{\text{cl}}^{\text{max}} = 0.746 \log \text{SFR} + 4.93. \quad (3)$$

We limit<sup>1</sup>  $M_{\text{cl}}^{\text{max}}$  to  $2 \times 10^7 M_{\odot}$ , and the mass of the smallest star cluster is set to  $M_{\text{cl}}^{\text{min}} = 5 M_{\odot}$  corresponding to individual groups in the Taurus-Auriga complex (Kroupa & Bouvier 2003). At the same time, it is possible to numerically derive the value of the largest stellar mass ( $m_{\text{max}}$ ) forming in a cluster, by imposing that it contains exactly one  $m_{\text{max}}$  star and using the universal IMF hypothesis. Pflamm-Altenburg et al. (2007) proposed the following fit to the numerical solution:

$$\log m_{\star}^{\text{max}} = 2.56 \log M_{\text{cl}} \times [3.82^{9.17} + (\log M_{\text{cl}})^{9.17}]^{1/9.17} - 0.38. \quad (4)$$

Observational data from Gunawardhana et al. (2011) require a stronger flattening of the galaxy-wide mass function slope at large SFRs with respect to what is inferred from the previous equations. To explain this result, Weidner et al. (2013) assumed that the  $\beta$  slope in Eq. 2 is not universal, but it also depends on SFR:

$$\beta = \begin{cases} 2 & \text{SFR} < 1 M_{\odot}/\text{yr} \\ -1.06 \log \text{SFR} + 2 & \text{SFR} \geq 1 M_{\odot}/\text{yr} \end{cases} \quad (5)$$

Possible variations of the high-mass end  $\alpha_3$  of the universal IMF in individual MCs as a function of cluster core density ( $\rho_{\text{cl}}$ ) and/or metallicity have been reported by a number of authors (see e.g. Kroupa et al. 2013, and references therein). Marks et al. (2012) used a principal component analysis to disentangle among the different possible choices. In the following, we adopt their proposed dependence of  $\alpha_3$  on  $\rho_{\text{cl}}$ :

$$\alpha_3 = \begin{cases} 2.35 & \rho_{\text{cl}} < 9.5 \times 10^4 M_{\odot}/\text{pc}^3 \\ 1.86 - 0.43 \log(\frac{\rho_{\text{cl}}}{10^4}) & \rho_{\text{cl}} \geq 9.5 \times 10^4 M_{\odot}/\text{pc}^3 \end{cases} \quad (6)$$

which has the advantage of being independent of metallicity. It is possible to theoretically derive the dependence of  $\rho_{\text{cl}}$  on  $M_{\text{cl}}$  (Marks & Kroupa 2012):

$$\log \rho_{\text{cl}} = 0.61 \log M_{\text{cl}} + 2.85 \quad (7)$$

Combining Eq. 1 to 7, the IGIMF  $\varphi_{\text{IGIMF}}$  is then defined as (see also Weidner & Kroupa 2005):

$$\varphi_{\text{IGIMF}}(m) = \int_{M_{\text{cl}}^{\text{min}}}^{M_{\text{cl}}^{\text{max}}} \varphi_*(m \leq m_{\star}^{\text{max}}(M_{\text{cl}})) \varphi_{\text{CL}}(M_{\text{cl}}) dM_{\text{cl}} \quad (8)$$

We stress that in the chosen formulation all the relevant quantities depend on the value of the SFR, which is the only input quantity needed from the SAM. The IGIMFs corresponding to 5 different choices of SFR, normalised to  $1 M_{\odot}$ , are shown in Fig. 1: while the shape at  $m_{\star} < 1 M_{\odot}$  is common, large deviations from the universal  $\varphi_{\star}$  are seen at most SFRs, with the lowest (highest) levels corresponding to IGIMFs bottom-heavier (top-heavier) than Kroupa (2001).

Using the theory depicted above it is possible to construct the IGIMF corresponding to each SFR episode during the evolution of model galaxies. However, the explicit computation of the IMF at each integration timestep, and for each model galaxy, would result in a relevant increase of the computational costs, thus losing one of the main advantages of the SAM approach. To avoid this problem, we compute the shape of IGIMF on a logarithmic grid of 21 SFR values covering the range  $-5 < \log \text{SFR} < 5$  with a  $0.5 \text{ dex}$  spacing and use the resulting IGIMF to compute the key quantities needed for our model (see next section for more details). While running our models, we will thus assign to each SFR event the IGIMF corresponding to the closest bin in logarithmic space (if the value lies exactly in between two values, we will assign the IGIMF corresponding to the lower one).

To better handle the shape of the IGIMF we fit it using a multi component power-law consistent with an extension of the Kroupa (2001) IMF. In fact, the usual three-slopes approximation (Eq. 1, where  $\alpha_3$  represents the slope fitted at high masses) is generally not enough for an acceptable fit and we introduce a fourth slope ( $\alpha_4$ ) at the high-mass end (which implies a new break mass  $m > m_1$ ). The usual choice  $m_1 = 1$  does not correctly reproduce the position of the second break mass in our formulation, for  $\text{SFR} < 1 M_{\odot}/\text{yr}$ : in this  $\text{SFR}$  range we then treat  $m_1$  as a free parameter. Finally, we impose  $m_{\text{max}} = 100 M_{\odot}$  for consistency with previous studies. The results of the fitting procedure are shown in Fig. 1 as dashed lines. The actual parameters for all binned SFR value considered are listed in Table 1.

<sup>1</sup> Our results do not depend on the exact choice for the upper limit cluster mass as Eq. 3 predicts  $M_{\text{cl}}^{\text{max}} > 2 \times 10^7 M_{\odot}$  only for values of  $\text{SFR} \gtrsim 10^{3.5} M_{\odot} \text{ yr}^{-1}$ , which never occur in our runs.

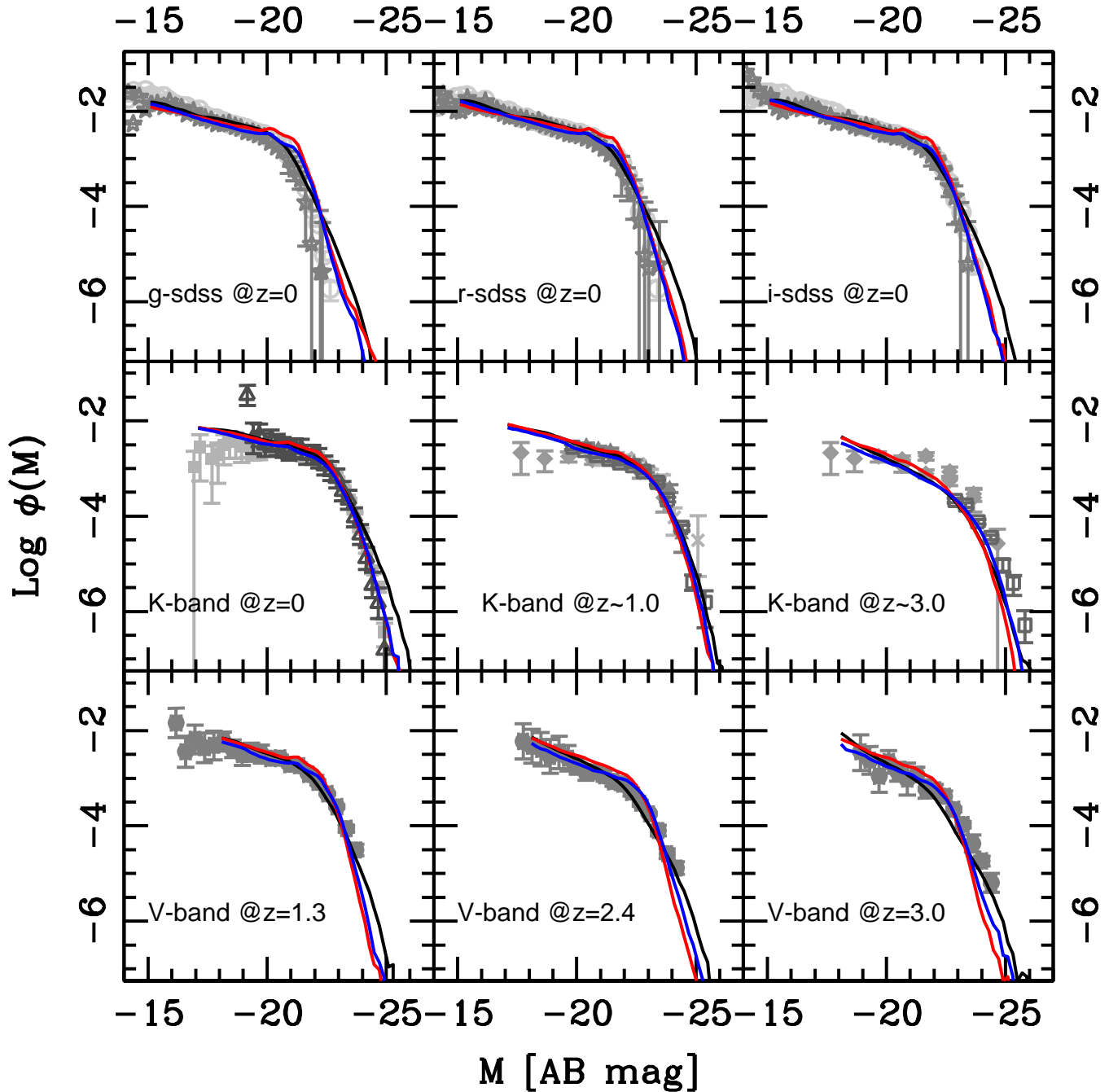


**Figure 2.** Predicted luminosity functions in different wavebands and at different redshifts. Solid black, red and blue lines refer to the predictions from the HDLF16, the Low- $\alpha_{SF}$  and High- $\alpha_{SF}$  models respectively. Grey symbols show observational estimates in the SDSS  $g$ ,  $r$  and  $i$ -bands by Blanton et al. (2005, empty circles) and Loveday et al. (2012, stars), in the  $K$ -band from Kochanek et al. (2001, empty triangles), Cole et al. (2001, filled squares), Pozzetti et al. (2003, crosses), Saracco et al. (2006, filled diamonds), Cirasuolo et al. (2010, empty squares) and in the  $V$ -band by Marchesini et al. (2012, filled circles). Models have been calibrated to reproduce the evolution of the  $K$  and  $V$ -band luminosity functions.

### 3 SEMI-ANALYTIC MODEL

We test the effect of the IGIMF on the evolution of chemical and physical properties of galaxies by including it in our semi-analytic model for Galaxy Evolution and Assembly (GAEA). This model represents an evolution of that described in De Lucia & Blaizot (2007), and it includes a detailed treatment of chemical enrichment (De Lucia et al. 2014) and an improved modeling of stellar feed-

back (Hirschmann et al. 2015, HDLF16 hereafter). Below, we give an overview of the key ingredients of the model. We refer the interested reader to the original papers for more details.

Galaxies are assumed to form from gas condensation at the centre of dark matter haloes, whose evolution is traced using  $N$ -body cosmological simulations. Galaxy evolution results from a complex network of physical processes including the cooling and heating of baryonic gas, star formation, accretion of gas onto Super-



**Table 1.** Analytical fits to the IGIMF corresponding to different star formation rates.

$\log SFR$ [ $M_{\odot}/\text{yr}$ ]	$m_1$ [ $M_{\odot}$ ]	$\alpha'_3$	$m_{\text{break}}$ [ $M_{\odot}$ ]	$\alpha'_4$	$m_{\text{max}}$ [ $M_{\odot}$ ]
-5.0	1.200	4.422	2.276	19.474	2.64
-4.5	1.288	3.817	3.914	16.923	4.72
-4.0	1.288	3.408	6.574	13.926	8.36
-3.5	1.286	3.179	11.087	12.227	14.79
-3.0	1.288	3.038	18.754	11.063	26.05
-2.5	1.287	2.937	30.972	10.412	44.16
-2.0	1.287	2.861	49.022	10.421	69.61
-1.5	1.287	2.766	76.816	12.991	97.87
-1.0	1.288	2.614	60.522	3.551	100
-0.5	1.170	2.516	74.030	3.012	100
0.0	1	2.458	9.994	2.387	100
0.5	1	2.354	11.774	2.214	100
1.0	1	2.250	11.536	2.068	100
1.5	1	2.142	10.846	1.937	100
2.0	1	2.033	10.137	1.817	100
2.5	1	1.921	9.526	1.703	100
3.0	1	1.807	9.066	1.592	100
3.5	1	1.731	8.833	1.538	100
4.0	1	1.684	8.756	1.518	100
4.5	1	1.644	8.725	1.500	100
5.0	1	1.609	8.746	1.485	100

Massive Black Holes (SMBHs) and the related feedback processes. In SAMs, these processes are modelled using analytical and/or numerical prescriptions that are observationally and/or theoretically motivated. Given the flexibility and affordable computational costs (with respect to cosmological hydrodynamical simulations) of this approach, it allows an efficient sampling of the parameter space, and a quantitative comparison of its predictions with available observational data.

In the following we will consider predictions from our modified version of the GAEA model. Most of the prescriptions included in this model are borrowed from De Lucia & Blaizot (2007), with modifications to follow more accurately processes on the scale of the Milky Way satellites, as described in De Lucia & Helmi (2008) and Li et al. (2010).

A significant update has been described in De Lucia et al. (2014), who introduced a new modeling for the chemical enrichment. This new scheme discards the simplified prescription of instantaneous recycling approximation and takes into account explicitly the dependence of stellar evolution on stellar mass. GAEA thus traces the evolution of individual chemical species accounting for finite stellar lifetimes and differential yields. Briefly, the model assumes stellar lifetimes parametrizations from Padovani & Matteucci (1993). Stars with  $m_{\star} < 8M_{\odot}$  enrich the ISM mainly in their Asymptotic Giant Branch (AGB) phase: for this population we use the yields from Karakas (2010). More massive stars are assumed to explode as Type II SNe releasing metals following the yields by Chieffi & Limongi (2002). The standard GAEA model assumes a delay time distribution for type Ia progenitors corresponding to the single degenerate scenario of Matteucci & Recchi (2001) and the Thielemann et al. (2003) metal yields. The probability of a given SNIa scenario is the only free parameter of the GAEA chemical scheme and, once the chemical yields for individual stars are defined, the global metal yield of a single stellar population as a function of time is uniquely predicted by the model (and not treated as a free parameter).

The second key improvement lies in the updated modeling of stellar feedback presented in HDLF16. In this paper, different parametrizations for stellar feedback have been extensively discussed and compared, with the aim of understanding their impact on the assembly of galaxies of different stellar mass, in particular with respect to the delayed formation/evolution of low-mass galaxies compared to massive ones. Results from HDLF16 show that some form of preventive or ejective feedback is needed in order to reproduce the significant evolution of galaxies below the knee of the stellar mass function. In this paper, we focus on just one of these feedback schemes, namely the one implementing the scalings derived from the “Feedback In Realistic Environments” (FIRE) simulation suite (Hopkins et al. 2014). These “zoom-in” hydrodynamic simulations include sub-grid models that account for individual sources of stellar feedback (i.e. energy and momentum input from SN explosions, radiative feedback and stellar winds) and are able to reproduce the baryon conversion efficiencies at different redshifts. In HDLF16 we adopt the analytical parametrization for gas reheating proposed by Muratov et al. (2015) as a fit to simulation results. In this parametrization, the reheating rate depends on both redshift and the maximum circular velocity of the gas, or only on the stellar mass (with hardly any redshift dependence). Outflow rates are estimated adopting the same formulation as in Guo et al. (2011), and gas reincorporation is modelled as in Henriques et al. (2013) assuming an explicit dependence of the reincorporation time-scale on halo mass. HDLF16 show that this model is able to reproduce the evolution of the galaxy stellar mass function, gas fractions and mass-metallicity relation.

In the following, we will refer to the HDLF16 predictions based on this feedback scheme as the *FIRE* model. For consistency, the same feedback scheme is adopted also in the IGIMF runs. It is worth noting here that the FIRE hydrodynamic simulations have been carried out assuming a universal IMF. This approach does not allow us to compute in a fully self-consistent way the rate and amount of energy injected into the inter-stellar medium, which depends on the assumed IMF. We note, however, that the adopted scalings allow us to reproduce the observed evolution of the galaxy stellar mass function also in the framework of the IGIMF theory (see below).

### 3.1 Modifications with respect to HDLF16

As discussed above, assuming an IGIMF requires associating a SFR-dependent IMF to each model galaxy, i.e. a different IMF needs to be selected for each episode of star formation (including those triggered by mergers). The implementation of this approach in GAEA requires some modifications of the code with respect to the HDLF16 version. The varying shape of the IGIMF affects primarily the baryonic mass fraction locked in low-mass stars (thus the total stellar mass, the luminosity and the metallicity of the galaxies), the number of SNe (thus the strength of stellar feedback), and the different ratio of Type Ia and Type II SNe (thus the abundance patterns of different gas phases and stars).

In the framework of the HDLF16 model, the IMF enters in two places:

- the amount of metals and energy restored into the ISM are computed using look-up tables that contain the amount of each chemical element considered (including H and He) and energy produced by SSP of  $1 M_{\odot}$  and distributed according to a Chabrier IMF (see De Lucia et al. 2014, for details). To generalise the approach, we construct a suite of tables corresponding to each of the IMF

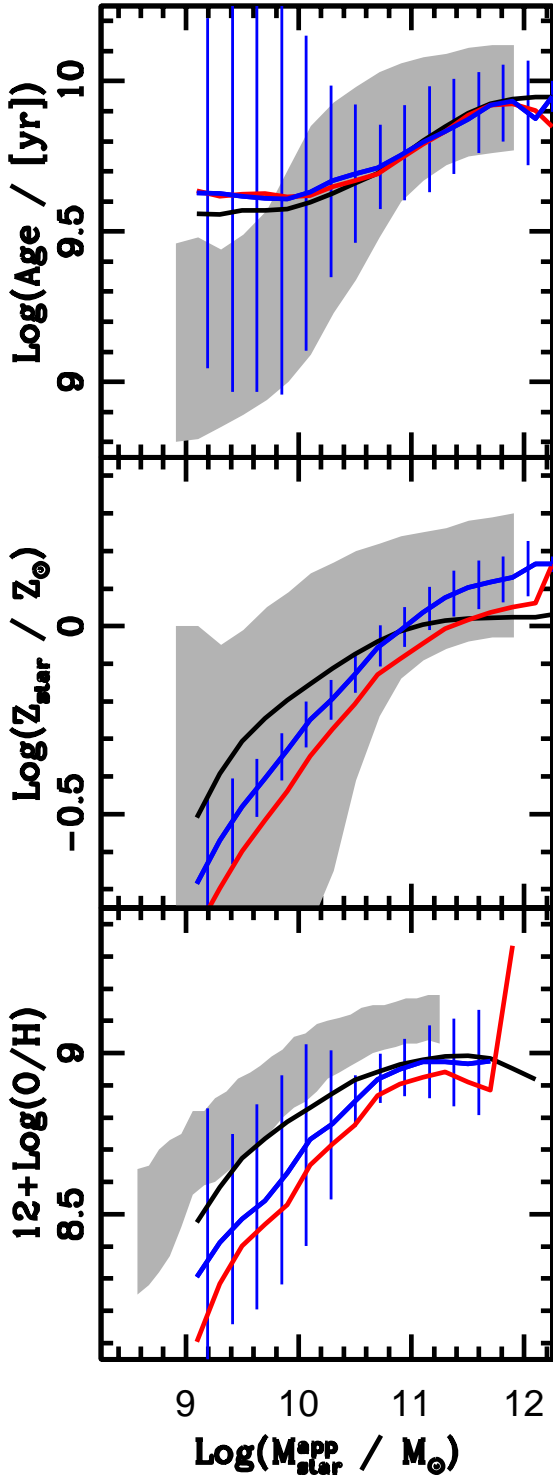


**Figure 3.** Local galaxy properties as a function of photometrically estimated - Chabrier IMF equivalent - stellar mass  $M_{\star}^{\text{app}}$ : *upper panel*:  $r$ -band luminosity-weighted ages; *middle panel*: total stellar metallicity; *lower panel*: cold gas metallicity. Black, red and blue lines represent the mean relations from the HDLF16, the Low- $\alpha_{\text{SF}}$  and High- $\alpha_{\text{SF}}$  models respectively, while the hatched areas represent the  $1\text{-}\sigma$  scatter in the High- $\alpha_{\text{SF}}$  run. Shaded areas represents observational results from Gallazzi et al. (2005) and Tremonti et al. (2004), both based on SDSS.

**Table 2.** Parameter values adopted for the runs considered in this study.

Parameter	HDLF16	High- $\alpha_{\text{SF}}$ model	Low- $\alpha_{\text{SF}}$ model
$\alpha_{\text{SF}}$	0.03	0.19	0.1
$\epsilon_{\text{reheat}}$	0.3	0.575	0.885
$\epsilon_{\text{eject}}$	0.1	0.12	0.06
$\gamma_{\text{reinc}}$	1.0	1.0	0.68
$\kappa_{\text{radio}}/10^{-5}$	1.0	1.78	0.87

bins considered. Each star formation episode (both quiescent and merger driven) is then associated to the appropriate table.

- the photometric properties of galaxies are computed interpolating tables containing the luminosity of a single burst of fixed mass, as a function of the age and metallicity of the stellar population and with a fixed IMF (see De Lucia et al. 2004, for details). Dust-extinguished magnitudes and luminosities are computed using the same approach as in De Lucia & Blaizot (2007). As above, we have constructed a set of tables corresponding to each IMF bin using an updated version of the Bruzual & Charlot (2003) models (G. Bruzual & S. Charlot, in preparation), which include the (Marigo et al. 2008) prescription for the evolution of thermally pulsing AGB (TP-AGB) stars.

### 3.2 Runs and calibrations

In this work, we run GAEA on merger trees extracted from the Millennium Simulation (Springel et al. 2005). This simulation assumes a  $\Lambda$ CDM concordance model, with parameters derived from WMAP1 (i.e.  $\Omega_{\Lambda} = 0.75$ ,  $\Omega_m = 0.25$ ,  $\Omega_b = 0.045$ ,  $n = 1$ ,  $\sigma_8 = 0.9$ ,  $H_0 = 73 \text{ km/s/Mpc}$ ). Although more recent measurements (Planck Collaboration XVI 2014) revise these values, we do not expect the differences in the cosmological parameters to change our main conclusions, as a minor retuning of the SAM parameters is usually enough to recover the same level of agreement with data (Wang et al. 2008; Guo et al. 2013).

Given the relevant changes induced in galaxy evolution due to the assumption of a SFR-dependent IGIMF, we recalibrate GAEA. The parameter set used in HDLF16 was tuned on the evolution of the galaxy stellar mass function. However, most of the estimates for physical quantities like  $M_{\star}$  and  $SFR$  based on photometry and/or spectroscopy are derived under the assumption of a universal IMF: therefore they cannot be used for calibrating our version of the SAM implementing the IGIMF. The only consistent tuning of our model can be obtained by comparing its predictions with direct (not derived) observational constraints, i.e. the luminosity functions (LFs).

The observational set used for calibration includes the evolution of the  $K$ -band LF (Kochanek et al. 2001; Cole et al. 2001; Pozzetti et al. 2003; Saracco et al. 2006; Cirasuolo et al. 2010) and the evolution of the  $V$ -band LF (Marchesini et al. 2012) at  $z \lesssim 3$ . We show the result of the recalibration procedure in Fig. 2, together with the  $z = 0$  LFs in the Sloan Digital Sky Survey (SDSS)  $g$ ,  $r$  and  $i$ -bands (Blanton et al. 2005; Loveday et al. 2012). To recover a good agreement with the data for the LFs in IGIMF version of GAEA, we have to modify the parameters governing SFR efficiency ( $\alpha_{\text{SF}}$ ), AGN feedback ( $\kappa_{\text{radio}}$ ), stellar feedback reheating ( $\epsilon_{\text{reheat}}$ ) and ejection rate ( $\epsilon_{\text{eject}}$ ), and the reincorporation rates ( $\gamma_{\text{reinc}}$ ).

We obtain good fits for the chosen LFs in a relatively large area of the parameter space, typically for star formation efficiencies in the range from  $\sim 10$  to  $\sim 20$  per cent. In the following, we

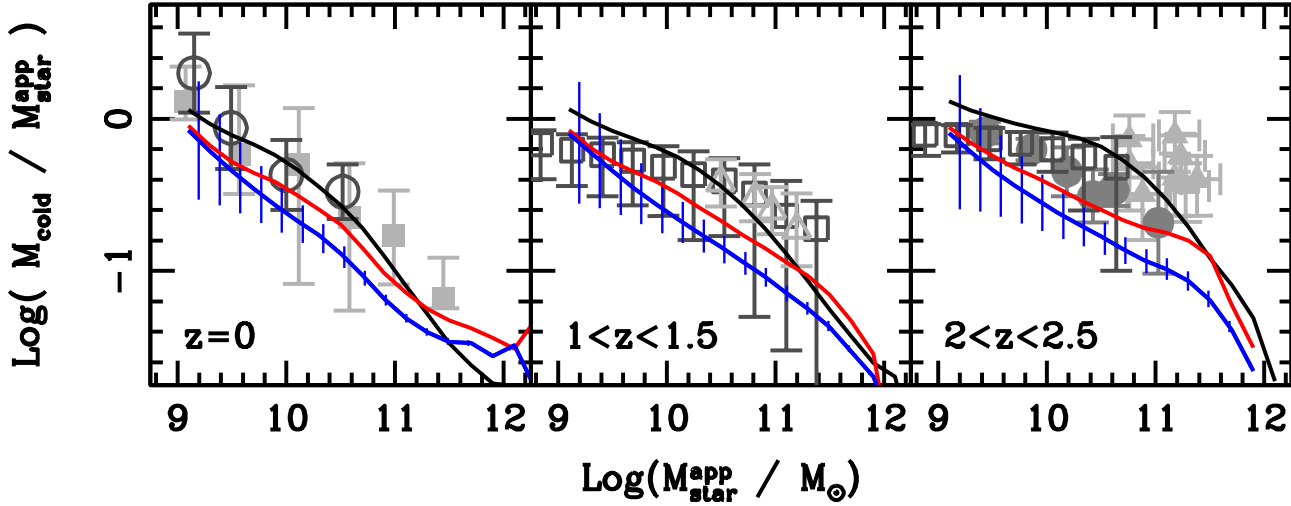


**Figure 4.** Redshift evolution of the cold gas fraction ( $M_{\text{cold}}/M_{\text{star}}^{\text{app}}$ ) of star-forming galaxies ( $SFR/M_{\text{star}}^{\text{app}} > 10^{-2} \text{ Gyr}^{-1}$ ). Lines, colours and hatched areas represent mean relations as in Fig. 3. Grey points refer to the data from Erb et al. (2006, filled circles), Tacconi et al. (2010, filled triangles), Tacconi et al. (2013, empty triangles), Peeples et al. (2014, filled squares), Boselli et al. (2014, empty circles) and Popping et al. (2015, empty squares).

show predictions for the two extreme runs (High- $\alpha_{\text{SF}}$  and Low- $\alpha_{\text{SF}}$ ), roughly covering this range of star formation efficiencies. The values of the relevant parameters for these two runs are listed in Table 2, along with those used in the HDLF16 model.  $\epsilon_{\text{reheat}}$  is larger in both IGIMF realizations than in the reference run. In the Low- $\alpha_{\text{SF}}$ , all efficiencies but  $\epsilon_{\text{reheat}}$  are smaller than the reference values, while in the High- $\alpha_{\text{SF}}$ , they are larger than in HDLF16. No additional calibration on the metal distributions has been performed with respect to HDLF16, so that all the plots showing abundance ratios are genuine predictions of the new GAEA version. Whenever stellar masses are estimated from photometry or spectroscopy (either SED-fitting procedures or colour based scalings), it could be problematic to compare them with the *true* stellar mass ( $M_{\star}$ ) predicted by GAEA, that depends on the star formation history of the model galaxy, via the IGIMF theory.

Therefore, we define an *apparent* - Chabrier (2003) IMF equivalent - stellar mass ( $M_{\star}^{\text{app}}$ ) from synthetic magnitudes using a mass-to-light vs colour relation as commonly done in the observational literature. We choose to work with the SDSS  $i$ -band and  $g - i$  as colour, following the results by, e.g., Zibetti et al. (2009, ZCR09 hereafter). In particular, we adopt the following relation:

$$\log \Upsilon_i = v(g - i) + \delta \quad (9)$$

where  $\Upsilon_i$  represents the stellar mass-to-light ratio in the  $i$ -band and  $v = 0.90$  and  $\delta = 0.70$  are best-fit coefficients derived as in Zibetti et al. (in prep.) from a Monte Carlo library of 500,000 synthetic stellar population spectra, in a similar way as in ZCR09. In detail, this library is also based on the revised version of the Bruzual & Charlot (2003) SSPs, that includes an improved treatment of the stellar remnants and of the TP-AGB evolutionary stage. Dust is treated using the Charlot & Fall (2000) 2-component prescription, in which enhanced attenuation is applied to young stars still residing in their birth clouds. With respect to ZCR09,

the new library covers an expanded range of star formations histories, including raising ones, and implements a simple prescription for chemical enrichment (a fixed stellar metallicity is assumed for each model in ZCR09). As a consistency check we compare  $M_{\star}^{\text{app}}$  and  $M_{\star}$  for the HDLF16 run with universal IMF. The two quantities are tightly correlated, but  $M_{\star}^{\text{app}}$  shows a constant shift with respect to  $M_{\star}$  of the order of 0.1 dex. ZCR09 show that a similar shift may be explained by spatial resolution effects:  $M_{\star}$  estimated from integrated photometry is systematically lower than the stellar mass obtained from resolved photometry because younger and less dust-obscured regions dominate the light and bias colours blue, hence the mass-to-light ratios low. Although ZCR09 does not have a statistical sample for a quantitative assessment of this effect, preliminary results from a sample of a few hundreds CALIFA<sup>2</sup> (Sánchez et al. 2012; Walcher et al. 2014) galaxies confirm the effect with an amplitude very similar to the one found here. Therefore, in all runs we compensate for this by adding to  $\delta$  an additional shift of 0.13. This formulation implies that using  $M_{\star}^{\text{app}}$  or  $M_{\star}$  is equivalent in HDLF16 (in a statistical sense, i.e. modulo some scatter).

## 4 RESULTS & DISCUSSION

### 4.1 Basic Predictions

In Fig 3, we show the relations between the luminosity-weighted stellar age (top panel), stellar metallicity (middle panel), cold gas metallicity (bottom panel) and stellar mass. As the stellar masses used in the observational relations (Tremonti et al. 2004;

<sup>2</sup> Calar Alto Legacy Integral Field spectroscopy Area survey

Gallazzi et al. 2005) are based on photometric estimates (e.g. SED-fitting), we use our apparent stellar masses  $M_{\star}^{\text{app}}$  for the comparison. In all panels in Fig. 3, the black solid line refers to the predictions of the HDLF16 model, while the red and blue lines to the predictions of our IGIMF-based GAEA realizations. Qualitatively, the IGIMF does not affect significantly any of the considered trends. The  $z = 0$  mass-metallicity relations tend to be somewhat steeper for the IGIMF runs than in the reference model, which is mainly due to low-mass galaxies being less enriched. It is worth stressing that the normalization of the observed mass-(cold gas) metallicity relation depends on the metallicity tracer used and the overall consistency among different estimates is of the order of  $\sim 0.2$  dex (Kewley & Ellison 2008). Considered that Tremonti et al. (2004) use a tracer biased in favour of high oxygen abundances, our predictions are still compatible with the data. The very steep relation found in the IGIMF runs is a potential issue, as the Tremonti et al. (2004) mass-metallicity relation is the steepest among the various observational determinations. We defer a more detailed analysis of the mass-metallicity relation (and its redshift-evolution), to a future work (De Lucia et al., in preparation).

Another relevant test for our IGIMF runs involves the amount of cold gas associated with model galaxies. In Fig. 4 we show the redshift evolution of the cold gas fraction ( $M_{\text{cold}}/M_{\star}^{\text{app}}$ ) of star-forming galaxies (defined as  $SFR/M_{\star}^{\text{app}} > 10^{-2} \text{ Gyr}^{-1}$ ). At fixed  $M_{\star}^{\text{app}}$ , both IGIMF runs predict gas fractions that are systematically lower than those predicted by the HDLF16 model, with a clear trend for decreasing fractions at increasing  $\alpha_{\text{SF}}$ . This behaviour is expected, as the larger SFR efficiencies in the IGIMF runs correspond to stronger reheating efficiencies, which deplete the cold gas more effectively. The Low- $\alpha_{\text{SF}}$  run formally provides the best-fit to the data; however, none of the models is ruled out by the available data, as the observational uncertainties are large.

#### 4.2 [O/Fe] ratios.

We then consider the  $[\alpha/\text{Fe}]$ -mass relation in early-type galaxies (Fig. 5). We compare<sup>3</sup> the mean  $[\text{O}/\text{Fe}]$  versus stellar mass relation in model galaxies with bulge-to-total ratios  $B/T > 0.7$  with the observational determinations for samples of local elliptical galaxies from Arrigoni et al. (2010), Spolaor et al. (2010), Thomas et al. (2010) and Johansson et al. (2012). Abundance ratios are typically estimated comparing spectral indexes (mainly Lick indexes) with predictions from evolutionary spectral synthesis codes. The calibration of these codes is critical for the correct recovery of element abundances. As an example, in Fig. 5 we show the estimates from Thomas et al. (2010, contours and dot-dashed line) and Johansson et al. (2012, long-short dashed line). These two studies consider the same sample of  $3360$   $0.05 \leq z \leq 0.06$  early-type galaxies from the MOSES (Morphologically Selected Early- types in SDSS) catalogue, but they analysed the sample using different versions of the same stellar population synthesis code (Maraston 2005). The difference in the results is driven by the different calibration adopted for the synthetic indexes (either based on globular clusters data or on flux-calibrated stellar libraries, see Thomas et al. 2011 for more details), which impacts both the normalization and

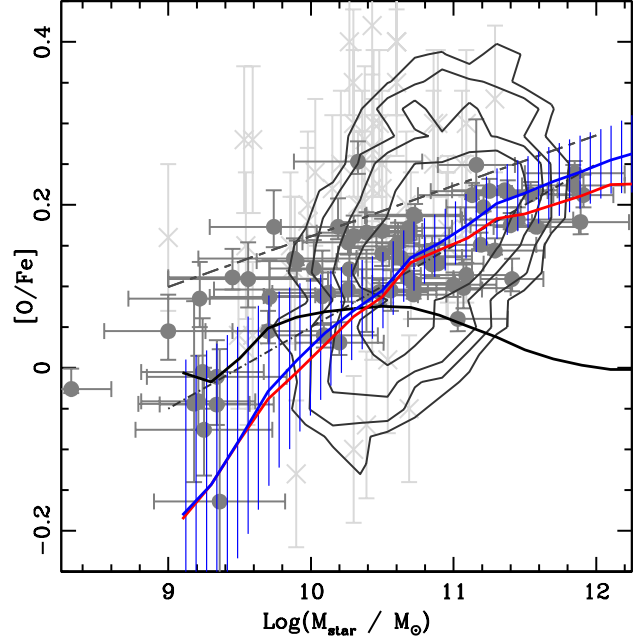


**Figure 5.**  $[\text{O}/\text{Fe}]$  ratios as predicted by GAEA compared to observed  $[\alpha/\text{Fe}]$  ratios for local elliptical galaxies. Lines, colours and hatched area are as in Fig. 3 (only model galaxies with  $B/T > 0.7$  have been included in the sample). Grey symbols and contours represent data from Arrigoni et al. (2010, dark grey circles), Thomas et al. (2010, contours and dot-dashed line), Spolaor et al. (2010, light grey crosses) and Johansson et al. (2012, long-short dashed line).

slope of the  $[\alpha/\text{Fe}]$ -mass relation. The Thomas et al. (2010) estimate is in good agreement with the data in Arrigoni et al. (2010), who present a re-analysis of the data in Trager et al. (2000), using a different stellar population synthesis method (i.e. Trager et al. 2008). All available measurements are obtained comparing data with synthetic spectra derived under the universal IMF assumption; however, we do not expect the systematic deviation due to the IGIMF to be larger than 0.1 dex (Recchi et al. 2009).

Stellar masses for individual sources in these datasets are derived from measured velocity dispersions and formally represent dynamical mass estimates. They are thus different from the proper  $M_{\star}$  predicted by our models. Nonetheless, we do not expect this mismatch to affect our main conclusion, as the stellar mass within one effective radius is a good proxy of dynamical mass for an early type galaxy (Cappellari et al. 2006). The shape of the predicted  $[\alpha/\text{Fe}]$ -mass relation is robust also if we consider  $M_{\star}^{\text{app}}$ . We remind that we did not require our model to fit this relation as a part of the recalibration procedure. The uncalibrated model (i.e. a model including the IGIMF, but using the same parameters as HDLF16) shows the same positive trend of  $[\alpha/\text{Fe}]$  with stellar mass. We also note that a similar  $[\text{O}/\text{Fe}]$ -mass relation holds for the whole galaxy population, not only for ellipticals galaxies.

While galaxies in HDLF16 are characterized by a flat distribution of  $[\text{O}/\text{Fe}]$ , our new version of GAEA nicely recovers the observed trend. The hatched blue region marks the  $1-\sigma$  scatter around the mean relation in the High- $\alpha_{\text{SF}}$  run, and is representative of the scatter in all our runs. Predictions from the IGIMF runs are in good agreement with the Arrigoni et al. (2010) and Thomas et al. (2010) samples, while they show a systematic offset from the more recent analysis by Johansson et al. (2012). The Spolaor et al. (2010) sam-

<sup>3</sup> In the following we will refer to  $[\alpha/\text{Fe}]$  ratios for the observational data and to the  $[\text{O}/\text{Fe}]$  for theoretical predictions. The rationale beyond this choice lies in the fact that, even if most of the observational estimates for  $[\alpha/\text{Fe}]$  are calibrated using Magnesium lines, Oxygen represents the most abundant among  $\alpha$ -elements.



ple (based on data on early-type galaxies in the Fornax and Virgo clusters) exhibit a larger scatter with respect to both our model predictions and other observational datasets.

In order to investigate the physical origin of the trends predicted by our IGIMF runs, we consider two additional runs (for the High- $\alpha_{\text{SF}}$  parameter set), where we impose a Chabrier-IMF either at  $SFR < 1M_{\odot}/\text{yr}$  or at  $SFR > 1M_{\odot}/\text{yr}$ . In the former run, we observe the same increase of  $[\text{O}/\text{Fe}]$  for  $M_{\star} \gtrsim 10^{10}M_{\odot}$  as in the High- $\alpha_{\text{SF}}$  case, while lower mass galaxies show the same level of  $[\text{O}/\text{Fe}]$  as in the reference HDLF16 run. Viceversa, in the latter run,  $M_{\star} \gtrsim 10^{10}M_{\odot}$  galaxies show the same flat distribution as in HDLF16, while lower mass galaxies are characterized by a decrease in  $[\text{O}/\text{Fe}]$ . We then conclude that the increase in  $\alpha$ -enhancement for massive galaxies is due to the IMF being top-heavier than Chabrier in their high- $\alpha_{\text{SF}}$  events, and viceversa, the decrease of the  $[\alpha/\text{Fe}]$  ratio in low-mass galaxies is due to these objects being dominated by IMFs bottom-heavier than Chabrier. This result is consistent with the similar analysis performed in G15, computing the mean high-stellar mass slopes for the IMFs associated with galaxies of different stellar mass. In their Fig. 5 they show that galaxies of increasing stellar mass are characterized by mean slopes increasingly top-heavier than low-mass counterparts. Although we use the same functional form for the universal IMF in individual stellar clusters (Eq. 1), our IGIMF description features a four-sloped shape (Sec. 2), that better describes the high-mass trends. Therefore, we can not replicate the same analysis as in G15 with our models. Nonetheless, the comparison of our findings with G15 clearly show that the IGIMF approach provides consistent predictions among different SAMs.

It is interesting to compare our findings with previous results from Arrigoni et al. (2010), Calura & Menci (2011), Yates et al. (2013) and G15, who claimed agreement between their model predictions and the observed  $[\alpha/\text{Fe}]$ -stellar mass relation. These authors invoke different mechanisms to explain the success of their models. The SAM discussed in Arrigoni et al. (2010) requires a mildly top-heavy IMF (i.e.  $\alpha_3 = 1.15$ ) and a fraction of binaries that explode as SNe Ia of about 3 percent. Calura & Menci (2011) advocate that the combination of “fly-by” harassment (that triggers starburst, boosting the SFR at high-redshift) and AGN feedback (which efficiently quench the same starbursts) considerably enhance the  $[\alpha/\text{Fe}]$ -levels in massive galaxies. Yates et al. (2013) reproduce a positive slope for  $[\alpha/\text{Fe}]$ -stellar mass relation, consistent with the Johansson et al. (2012) estimate, using a universal (Chabrier-like) IMF and assuming that the prompt component in the SN-Ia delay-time distribution (DTD) is smaller than 50 percent. Finally, G15 implement an IGIMF model, which is rather similar to our approach: the main difference with our work is that they use the  $[\alpha/\text{Fe}]$ -mass relation for calibration, while in our approach this is a genuine prediction of the model. G15 find an almost flat  $[\alpha/\text{Fe}]$ -stellar mass relation for models adopting a universal Salpeter-like IMF, while obtaining a noticeable steepening of the relation for the IGIMF runs.

Predictions of our reference model are consistent with these results: our standard model based on a universal IMF predicts slopes for the  $[\alpha/\text{Fe}]$ -stellar mass relation which are too shallow. We also test the effect of different DTDs, and find that for all DTDs considered in De Lucia et al. (2014) the HDLF16 model predicts a flat relation (but with a different normalization). Given the fact that we do not calibrate our IGIMF runs on the  $[\text{O}/\text{Fe}]$ - $M_{\star}$  relation, the striking agreement of our predictions with observed data (even for the overall normalization of the relation) is remarkable. Although this success is not unique to our model, we note relevant differ-

ences with respect to previous work. First of all, our IGIMF runs predict the steepest slope for this relation. This effect is likely connected with the assumed variation of  $\beta$  for  $SFR > 1M_{\odot} \text{ yr}^{-1}$  (Eq. 5). We check this by computing the mean value of  $\beta$  for the integrated stellar populations corresponding to the typical star formation histories at different mass scales (weighted with the stellar mass formed at each epoch). We find a clear trend of decreasing  $\langle \beta \rangle$  with increasing  $M_{\star}$ , with  $\langle \beta \rangle = 2$  for low-mass galaxies and  $\langle \beta \rangle \sim 1.75$  for the highest mass galaxies in our cosmological sample. This effect was not considered in G15, who, however, tested the effect of a different (fixed)  $\beta$ , finding that smaller values correspond to steeper relations. Moreover, for stellar masses  $M_{\star} < 10^{10}M_{\odot}$  all models considered in G15 tend to predict positive mean  $[\text{O}/\text{Fe}]$ , with only a small fraction of the model galaxies showing negative ratios, while these negative ratios are found for a non-negligible fraction of both the Arrigoni et al. (2010) and Spolaor et al. (2010) samples. The actual fraction of galaxies below a given  $[\text{O}/\text{Fe}]$  threshold in GAEA depends on the overall normalization of the  $[\text{O}/\text{Fe}]$ - $M_{\star}$  relation. We have verified that in the IGIMF runs, the normalization of the relation (and weakly its slope) depends on the assumed DTD. This is due to the different amount of ‘prompt’ Fe released to the ISM (see e.g. the analysis in De Lucia et al. 2014).

We stress again that the IGIMF approach does not represent a unique solution for the  $[\alpha/\text{Fe}]$ -stellar mass conundrum in hierarchical models of galaxy formation and evolution. We discussed some alternative models earlier in this section. We also note that several authors claim that AGN feedback can play a big role in setting high  $[\alpha/\text{Fe}]$  ratio in massive galaxies via a sudden quenching of star formation (Pipino et al. 2009, Segers et al. 2016, Hirschmann et al. in preparation).

### 4.3 Assembly histories and stellar mass estimates

In the previous section, we discussed the implications of the IGIMF theory on the chemical enrichment properties of galaxies as predicted by GAEA. In this section, we complement this investigation with analysis of the effect on the distribution of stellar masses.

First of all we analyse the redshift evolution of the galaxy stellar mass function. For all runs considered, when the *true*  $M_{\star}$  is used, the predicted mass functions lie very close to those predicted by HDLF16. On the other hand, when the photometrically estimated, *apparent*  $M_{\star}^{\text{app}}$  is considered, the high-mass end predictions from the IGIMF runs systematically deviate from those of the HDLF16 model at  $z < 1$  (Fig. 6). Overall, the IGIMF runs are able to reproduce the evolution of the mass function as well as the reference HDLF16 runs, but the growth of the high mass-end of the mass function is somewhat slowed down at  $z \lesssim 1$ . Although the match between model predictions and data is still not perfect, a reduced growth rate in apparent  $M_{\star}^{\text{app}}$  for the most massive galaxies at low-redshifts is an intriguing result (see e.g. Cimatti et al. 2006; Monaco et al. 2006).

In order to better understand the effect of a non universal IMF on galaxy assembly, we contrast in Fig. 7 the evolution of key physical properties in the HDLF16 and High- $\alpha_{\text{SF}}$  IGIMF runs (similar results hold for the Low- $\alpha_{\text{SF}}$  IGIMF run) for model  $B/T > 0.7$  galaxies at four different  $z = 0$  mass bins ( $M_{\star} \sim 10^{12}, 10^{11.5}, 10^{10.5}$  and  $10^{9.25}M_{\odot}$ ). In detail, we consider the normalised star formation histories (upper panel), cumulative mass assembly (middle panel) and the mean  $[\text{O}/\text{Fe}]$  (lower panel). For each model galaxy, the contribution of all its progenitors has been included. Massive galaxies exhibit star formation histories peaking at higher

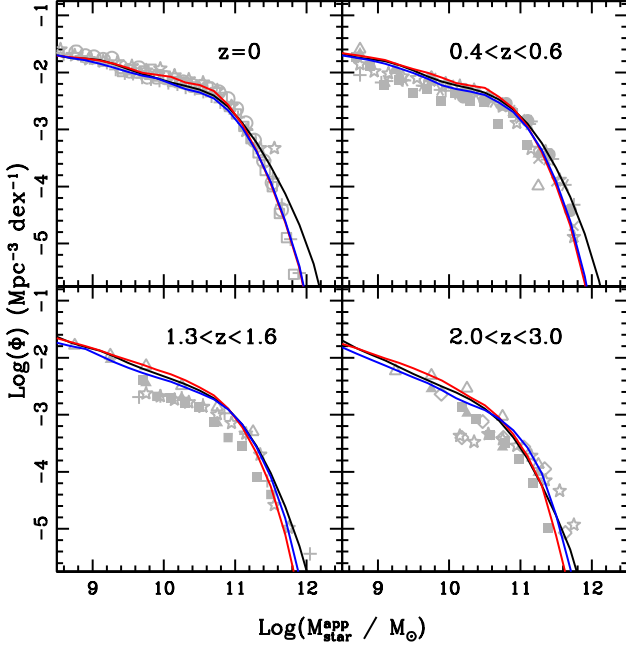


**Figure 6.** Redshift evolution of the galaxy stellar mass function, as a function of the apparent  $M_{\star}^{\text{app}}$ . Lines and colours are as in Fig. 2; grey points refer to the compilation from Fontanot et al. (2009, see references therein).

redshifts and a more rapid assembly with respect to their low-mass counterparts; this is consistent with results from De Lucia et al. (2006) and predictions based on the HDLF16 run. Therefore, the IGIMF scheme does not affect heavily the overall star formation histories and mass assembly histories of the different galaxy populations. The main difference is seen in the lower panel: as the stronger SFRs associated with more massive galaxies correspond to IGIMFs top-heavier than the universal IMF, this results into a stronger  $\alpha$ -enhancement at earlier epochs with respect to a model using a universal IMF. The later incorporation of larger amounts of Fe produced by SNIa, produces a dilution of the mean [O/Fe], but the tracks corresponding to the different mass scales remain independent. On the other hand, in the HDLF16 run, the level of initial  $\alpha$ -enhancement is reduced and late evolution tends to wash differences out, leading to an average [O/Fe] ratio that does not depend significantly on stellar mass. These results suggest that, using the IGIMF, the so-called “chemoarchaeological downsizing” naturally arise in a concordance cosmological model and that, under the IGIMF assumption,  $[\alpha/\text{Fe}]$  ratios are good tracers of the highest SFR events in galaxies of given mass, but they do not bear much information on the overall star formation timescales. In fact, at fixed  $z = 0$  stellar mass, the highest SFR events and the timescale of star formation are degenerate quantities, but the former is the dominant quantity to set the final level of  $\alpha$ -enhancement as a function of stellar mass. This can be best appreciated in the top-panels of Fig. 7: star formation timescales are shorter for more massive galaxies both in the HDLF16 and the IGIMF run, but only the latter realizations reach the required values of [O/Fe].

We then directly study the effect of the IGIMF on the stellar mass estimate. Independent analysis of early-type samples based either on dynamical modeling (Cappellari et al. 2012) or on spectral synthesis models (Conroy & van Dokkum 2012) suggest possible variations of the overall shape of the IMF in these galaxies. In

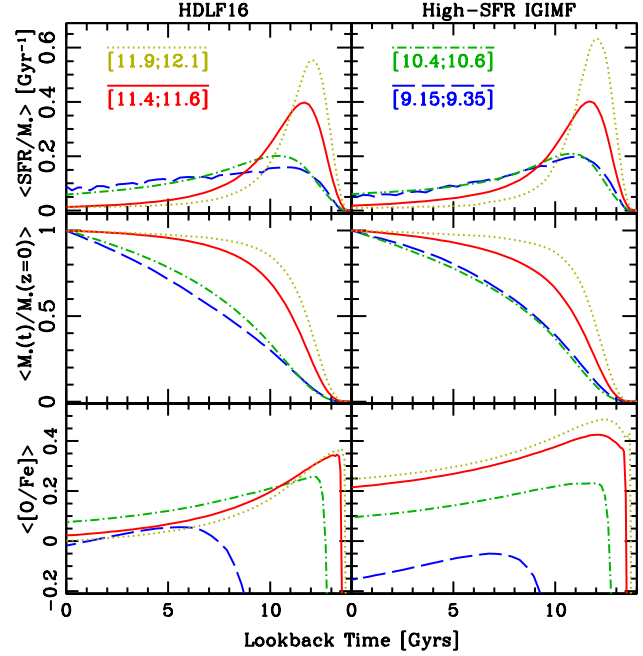


**Figure 7.** Mean evolutionary histories for galaxies in different  $\text{Log}(M/M_{\odot})$  intervals (as indicate in the caption) in the HDLF16 (left column) and High- $\alpha_{\text{SF}}$  (right column) runs. *Upper panels:* mean normalised star formation history; *middle panels:* cumulative mass assembly; *lower panels:* evolution of the [O/Fe] ratio.

particular, Cappellari et al. (2012) compare integral-field maps of stellar kinematics and optical imaging with dynamical models including both stellar and DM components. Conroy & van Dokkum (2012) consider a sample of compact early-type galaxies (so that  $\sigma$  is expected to be dominated by the stellar component, at least within the effective radius) and estimate mass-to-light ratios and stellar masses by fitting spectral features sensitive to the stellar effective temperature and surface gravity against stellar population synthesis models. Within this framework, they model the high- and low-mass end of the IMF as free parameters. They then compare the best-fit values for the physical properties with those derived assuming a universal MW-like IMF, and argue that the IMF in early-type galaxies becomes increasingly “bottom-heavy” (i.e. with a larger fraction of low mass stars with respect to the universal IMF) with increasing velocity dispersion ( $\sigma$ ) or galaxy stellar mass.

In the left panel of Fig. 8 we show the ratio of the proper stellar mass-to-light ratio in the  $i$ -band ( $M_{\star}/L_i$ ) and  $\Upsilon_i$ , derived using Eq. 9, as a function of the proper  $M_{\star}/L_i$ , as in the dynamical analysis of Cappellari et al. (2012). The right panel shows the  $M_{\star}/M_{\star}^{\text{app}}$  ratio, as a function of  $M_{\star}$ : this plot roughly corresponds to the analogous figure in Conroy et al. (2013). In both panels only bulge-dominated model galaxies (i.e.  $B/T > 0.7$ ) have been considered. In both panels of Fig. 8 predictions for the reference HDLF16 run are consistent with a flat relation, while the IGIMF runs suggest a larger mass-to-light ratio (left panel) and stellar mass (right panel) with respect to a Chabrier (2003) IMF<sup>4</sup> at increasing stellar mass and/or mass-to-light ratio. Model predictions are therefore in good qualitative agreement with the results of Cappellari et al. (2012)

<sup>4</sup> We neglect here the small difference in normalization between the Kroupa 2001 and the Chabrier 2003 IMF used for the  $M_{\star}^{\text{app}}$  calibration

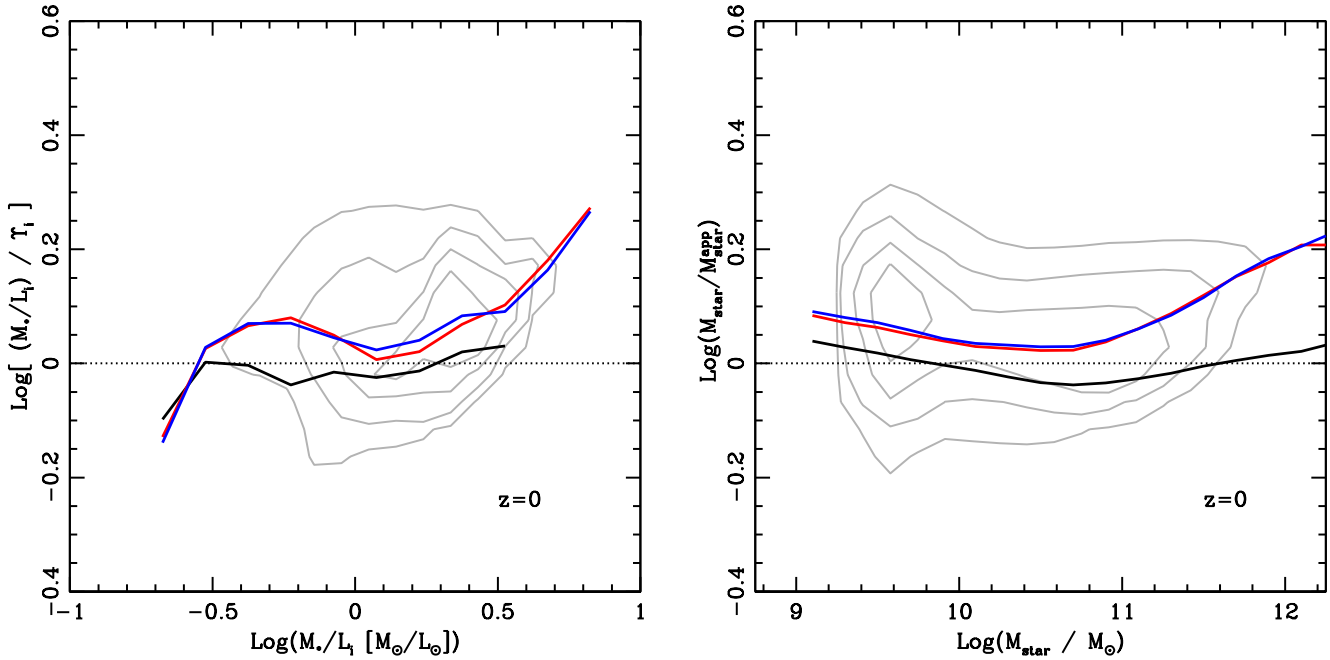


**Figure 8.** Deviations from the assumption of a universal Chabrier-like IMF for stellar mass (right panel) and stellar mass-to-light ratio (left panel). In each panel, lines and colours are as in Fig. 2; grey contours mark galaxy number densities levels (normalised to the maximum density) corresponding to 1, 10 and 50 percent in the High- $\alpha_{\text{SF}}$  IGIMF run.

and Conroy & van Dokkum (2012). Moreover, we notice the relevant scatter in the predicted relations, that may explain the results of Smith et al. (2015), who analyse two gravitationally lensed massive elliptical galaxies finding mass-to-light ratios consistent with a universal IMF (see also the recent results from Leier et al. 2015).

It is worth stressing that the comparison of our model predictions with data from Cappellari et al. (2012) and Conroy & van Dokkum (2012), can be only qualitative: a more quantitative comparison would require an attempt to replicate both the same selection criteria adopted in the observational studies and the same tracers for dynamical properties (like  $\sigma$ ). As a final note, we stress that Fig. 8 differs from the similar plot shown in Fontanot (2014, their Fig. 5). In this work, the photometrically-equivalent quantities are computed self-consistently from the predicted magnitudes in the IGIMF realisation, while in previous work the mass differences were computed comparing model galaxies in different realizations (with or without a universal IMF) on an object-by-object basis. The present approach provides a more stringent constrain on the expected mass deviations with respect to a local universal IMF.

## 5 CONCLUSIONS

This paper presents an updated version of the GAEA semi-analytic model of galaxy formation and evolution, which includes the effects of assuming that stars form following an IMF, whose shape depends on the instantaneous SFR levels (see e.g. Weidner et al. 2013). Coupled with the detailed chemical enrichment model introduced in De Lucia et al. (2014) and with the feedback scheme presented in Hirschmann et al. (2015), this version allows us to study the impact of this hypothesis on the galaxy mass assembly and its

imprint on the chemical abundances of both stars and cold gas in galaxies.

The different amount of stars locked in a low-mass and long-living population affects significantly the physical properties of model galaxies, and forces a recalibration of the key free parameters describing star formation and feedback. We choose to recalibrate our GAEA version requiring it to reproduce the redshift evolution of the  $K$  and  $V$  band luminosity functions. We then derive photometrically-equivalent stellar masses using an empirical relation between mass-to-light ratios and colours, calibrated using a large library of synthetic spectra built using a universal Chabrier (2003) IMF.

We show that this new model predicts local scalings of the luminosity-weighted age, stellar metallicity and cold gas metallicity with stellar mass in close agreement with the results of HDLF16. The main difference with previous versions of GAEA lies in the  $\alpha$ -enhancement of bulge-dominated galaxies: while HDLF16 predict a flat relation with stellar mass, our IGIMF-based model correctly reproduces the measured increase of  $[\alpha/\text{Fe}]$  ratios as a function of stellar mass. These results confirm early findings by G15 and show that the impact of the IGIMF approach is robust and independent of the details of the semi-analytic model in which it has been implemented. We also study the relation between the proper stellar masses predicted by our best run and the apparent stellar masses derived from synthetic photometry in the IGIMF runs, assuming a universal IMF. We show that, for high-mass galaxies, the  $M_*/M_*^{\text{app}}$  ratio is typically positive, with a relevant scatter. Similar conclusions hold for the corresponding ratio between the proper and apparent mass-to-light ratios. These predictions are in qualitative agreement with data from Cappellari et al. (2012) and Conroy & van Dokkum (2012). These groups find in their data an excess of mass-to-light ratio and stellar mass (respectively) with respect to what expected using a universal IMF

and interpret this discrepancy as an evidence in favour of a typical IMF “bottom-heavier” than the Chabrier or Kroupa IMF. In the framework of the IGIMF runs, the discrepancy between  $M_*$  and  $M_*^{\text{app}}$  is *not* due to an intrinsic “bottom-heavier” IMF in massive galaxies. In fact, our massive model galaxies are characterized by an effective IMF (i.e. the mean slopes computed over the typical star formation histories in Fig. 7) with high-mass slopes smaller than 2.35 (i.e. by a “top-heavy” IMF). Our conclusions are therefore in contrast with those by Cappellari et al. (2012) and Conroy & van Dokkum (2012), which we interpret as due to the mismatch between proper mass-to-light ratios and those derived from synthetic photometry, under the assumption of a universal IMF. The disagreement with Conroy & van Dokkum (2012) is particularly interesting, since these authors use spectral features sensitive to the ratio between low-mass stars and giants, but we cannot explicitly test these observables and quantify the level of disagreement, within our current model predictions.

We test the robustness of our results against a change in the modelling of mass and energy transfer between galaxy components (bulge, disc, halo) in galaxy mergers as proposed in Kannan et al. (2015). In Fontanot et al. (2015), we showed that these new prescriptions have a relevant impact on the distribution of galaxies in the different morphological types. We then run an additional realisation switching on Kannan et al. (2015) recipes and using the same parameters as in our IGIMF run (i.e. we did not attempt to recalibrate this model). All predictions shown in this paper are robust against this change in the merger modelling. The main difference we see is a slight increase of the  $[\alpha/\text{Fe}]$ -enhancement at both the low-mass and high-mass end, which brings model predictions in better agreement with the linear fit of Thomas et al. (2010). These changes are not driven by a different star formation history in this run, but from its different sample of “elliptical” ( $B/T > 0.7$ ) galaxies.

In this paper, we show for the first time a model which reproduces, *at the same time*, the evolution of the stellar mass function and the abundance patterns of elliptical galaxies, and explains the observed peculiar dynamical properties of local early type galaxies. Our model is, however, not without problems. For example, model galaxies below the knee of the mass function host stellar populations that are still too old (irrespective of the feedback scheme and treatment of satellite galaxies), indicating a disagreement between predicted and observationally estimated star formation histories at this mass scale.

As mentioned above, a varying IMF does not represent a unique solution to reproduce the observed trend of  $[\alpha/\text{Fe}]$  ratios in early-type galaxies: alternative solutions cannot be excluded and will be tested in future work. Among these, metal enriched winds represent an interesting option in the framework of strong ejective feedback models like that adopted in GAFA (see e.g. Yates et al. 2013). Robust constraints for different schemes can be obtained from the metal enrichment of the intergalactic medium, typically traced using quasar spectra (see e.g. D’Odorico et al. 2016 and references herein). On the other hand, dynamical studies provide the strongest indication in favour of a varying IMF hypothesis. While a more quantitative comparison of our model predictions with available data is beyond the aims of the present work, a better characterisation of the selection effects at play and a detailed modeling of physical quantities like  $\sigma$  are clearly required. Ongoing integral field spectroscopy observations of large samples of nearby galaxies

(e.g. MaNGA<sup>5</sup>, Bundy & et al. 2015, or the SAMI<sup>6</sup> Galaxy survey, Bryant & et al. 2015) will provide statistical support to the claimed excess of low-mass stars in massive galaxies.

## ACKNOWLEDGEMENTS

We thank P. Kroupa and J. Pflamm-Altenburg for enlightening discussions on the details of the IGIMF model and R. Yates for stimulating discussions. We thank the anonymous referee for useful comments that helped us improving the clarity of the manuscript. FF acknowledges financial support from the grant PRIN MIUR 2012 “The Intergalactic Medium as a probe of the growth of cosmic structures”. GDL acknowledges financial support from the MERAC foundation. FF and GDL also acknowledge from the grants PRIN INAF 2014 “Glittering kaleidoscopes in the sky: the multifaceted nature and role of Galaxy Clusters.” MH acknowledges financial support from the European Research Council via an Advanced Grant under grant agreement no. 321323 (NEOGAL). GB acknowledges support for this work from the National Autonomous University of México (UNAM), through grant PAPIIT IG100115. SZ has been supported by the EU Marie Curie Career Integration Grant “SteMaGE” Nr. PCIG12-GA-2012-326466 (Call Identifier: FP7-PEOPLE-2012 CIG)

## REFERENCES

- Arrigoni M., Trager S. C., Somerville R. S., Gibson B. K., 2010, *MNRAS*, 402, 173
- Blanton M. R., Lupton R. H., Schlegel D. J., Strauss M. A., Brinkmann J., Fukugita M., Loveday J., 2005, *ApJ*, 631, 208
- Boselli A., Cortese L., Boquien M., Boissier S., Catinella B., Lagos C., Saintonge A., 2014, *A&A*, 564, A66
- Bruzual G., Charlot S., 2003, *MNRAS*, 344, 1000
- Bryant J. J., et al. 2015, *MNRAS*, 447, 2857
- Bundy K., et al. 2015, *ApJ*, 798, 7
- Calura F., Menci N., 2011, *MNRAS*, 413, L1
- Cappellari M., Bacon R., Bureau M., Damen M. C., Davies R. L., de Zeeuw P. T., Emsellem E., Falcón-Barroso J., Krajnović D., Kuntschner H., McDermid R. M., Peletier R. F., Sarzi M., van den Bosch R. C. E., van de Ven G., 2006, *MNRAS*, 366, 1126
- Cappellari M., McDermid R. M., Alatalo K., Blitz L., Bois M., Bournaud F., Bureau M., Crocker A. F., et al. 2012, *Nature*, 484, 485
- Chabrier G., 2003, *ApJ*, 586, L133
- Chieffi A., Limongi M., 2002, *ApJ*, 577, 281
- Cimatti A., Daddi E., Renzini A., 2006, *A&A*, 453, L29
- Cirasuolo M., McLure R. J., Dunlop J. S., Almaini O., Foucaud S., Simpson C., 2010, *MNRAS*, 401, 1166
- Cole S., Norberg P., Baugh C. M., Frenk C. S., Bland-Hawthorn J., Bridges T., Cannon R., Colless M. e. a., 2001, *MNRAS*, 326, 255
- Conroy C., Dutton A. A., Graves G. J., Mendel J. T., van Dokkum P. G., 2013, *ApJ*, 776, L26
- Conroy C., van Dokkum P. G., 2012, *ApJ*, 760, 71
- Cora S. A., 2006, *MNRAS*, 368, 1540
- De Lucia G., Blaizot J., 2007, *MNRAS*, 375, 2

<sup>5</sup> Mapping Nearby Galaxies at Apache Point Observatory

<sup>6</sup> Sydney Australian Astronomical Observatory Multi-object Integral-Field Spectrograph



- De Lucia G., Helmi A., 2008, *MNRAS*, 391, 14
- De Lucia G., Kauffmann G., White S. D. M., 2004, *MNRAS*, 349, 1101
- De Lucia G., Springel V., White S. D. M., Croton D., Kauffmann G., 2006, *MNRAS*, 366, 499
- De Lucia G., Tornatore L., Frenk C. S., Helmi A., Navarro J. F., White S. D. M., 2014, *MNRAS*, 445, 970
- D’Odorico V., Cristiani S., Pomante E., Carswell R. F., Viel M., Barai P., Becker G. D., Calura F., Cupani G., Fontanot F., Haehnelt M. G., Kim T.-S., Miralda-Escudé J., Rorai A., Tescari E., Vanzella E., 2016, *MNRAS*
- Erb D. K., Shapley A. E., Pettini M., Steidel C. C., Reddy N. A., Adelberger K. L., 2006, *ApJ*, 644, 813
- Ferreras I., La Barbera F., de la Rosa I. G., Vazdekis A., de Carvalho R. R., Falcón-Barroso J., Ricciardelli E., 2013, *MNRAS*, 429, L15
- Fontanot F., 2014, *MNRAS*, 442, 3138
- Fontanot F., De Lucia G., Monaco P., Somerville R. S., Santini P., 2009, *MNRAS*, 397, 1776
- Fontanot F., Macciò A. V., Hirschmann M., De Lucia G., Kannan R., Somerville R. S., Wilman D., 2015, *MNRAS*, 451, 2968
- Gallazzi A., Charlot S., Brinchmann J., White S. D. M., Tremonti C. A., 2005, *MNRAS*, 362, 41
- Gargiulo I. D., Cora S. A., Padilla N. D., Muñoz Arancibia A. M., Ruiz A. N., Orsi A. A., Tecce T. E., Weidner C., Bruzual G., 2015, *MNRAS*, 446, 3820
- Gunawardhana M. L. P., Hopkins A. M., Sharp R. G., Brough S., Taylor E., Bland-Hawthorn J., Maraston C., Tuffs R. J., et al. 2011, *MNRAS*, 415, 1647
- Guo Q., White S., Angulo R. E., Henriques B., Lemson G., Boylan-Kolchin M., Thomas P., Short C., 2013, *MNRAS*, 428, 1351
- Guo Q., White S., Boylan-Kolchin M., De Lucia G., Kauffmann G., Lemson G., Li C., Springel V., Weinmann S., 2011, *MNRAS*, 413, 101
- Hennebelle P., Chabrier G., 2008, *ApJ*, 684, 395
- Henriques B. M. B., White S. D. M., Thomas P. A., Angulo R. E., Guo Q., Lemson G., Springel V., 2013, *MNRAS*, 431, 3373
- Hirschmann M., De Lucia G., Fontanot F., 2015, *ArXiv e-prints* (arXiv:1512.04531)
- Hopkins P. F., 2012, *MNRAS*, 423, 2037
- Hopkins P. F., Kereš D., Oñorbe J., Faucher-Giguère C.-A., Quataert E., Murray N., Bullock J. S., 2014, *MNRAS*, 445, 581
- Hoversten E. A., Glazebrook K., 2008, *ApJ*, 675, 163
- Johansson J., Thomas D., Maraston C., 2012, *MNRAS*, 421, 1908
- Kannan R., Macciò A. V., Fontanot F., Moster B. P., Karman W., Somerville R. S., 2015, *MNRAS*, 452, 4347
- Karakas A. I., 2010, *MNRAS*, 403, 1413
- Kewley L. J., Ellison S. L., 2008, *ApJ*, 681, 1183
- Klessen R. S., Ballesteros-Paredes J., Vázquez-Semadeni E., Durán-Rojas C., 2005, *ApJ*, 620, 786
- Klessen R. S., Spaans M., Jappsen A.-K., 2007, *MNRAS*, 374, L29
- Kochanek C. S., Pahre M. A., Falco E. E., Huchra J. P., Mader J., Jarrett T. H., Chester T., Cutri R., Schneider S. E., 2001, *ApJ*, 560, 566
- Kroupa P., 2001, *MNRAS*, 322, 231
- Kroupa P., Bouvier J., 2003, *MNRAS*, 346, 369
- Kroupa P., Weidner C., Pflamm-Altenburg J., Thies I., Dabringhausen J., Marks M., Maschberger T., 2013, *Planets, Stars and Stellar Systems. Volume 5: Galactic Structure and Stellar Populations*, 5, 115
- Krumholz M. R., 2014, *ArXiv e-prints* (arXiv:1402.0867)
- Lada C. J., Lada E. A., 2003, *ARA&A*, 41, 57
- Leier D., Ferreras I., Saha P., Charlot S., Bruzual G., La Barbera F., 2015, *ArXiv e-prints*
- Li Y.-S., De Lucia G., Helmi A., 2010, *MNRAS*, 401, 2036
- Loveday J., Norberg P., Baldry I. K., Driver S. P., Hopkins A. M., Peacock J. A., Bamford S. P., Liske J., et al. 2012, *MNRAS*, 420, 1239
- Maraston C., 2005, *MNRAS*, 362, 799
- Marchesini D., Stefanon M., Brammer G. B., Whitaker K. E., 2012, *ApJ*, 748, 126
- Marigo P., Girardi L., Bressan A., Groenewegen M. A. T., Silva L., Granato G. L., 2008, *A&A*, 482, 883
- Marks M., Kroupa P., 2012, *A&A*, 543, A8
- Marks M., Kroupa P., Dabringhausen J., Pawłowski M. S., 2012, *MNRAS*, 422, 2246
- Matteucci F., 1994, *A&A*, 288, 57
- Matteucci F., Recchi S., 2001, *ApJ*, 558, 351
- McWilliam A., Wallerstein G., Mottini M., 2013, *ApJ*, 778, 149
- Monaco P., Murante G., Borgani S., Fontanot F., 2006, *ApJ*, 652, L89
- Muratov A. L., Kereš D., Faucher-Giguère C.-A., Hopkins P. F., Quataert E., Murray N., 2015, *MNRAS*, 454, 2691
- Nagashima M., Lacey C. G., Okamoto T., Baugh C. M., Frenk C. S., Cole S., 2005, *MNRAS*, 363, L31
- Narayanan D., Davé R., 2013, *MNRAS*, 436, 2892
- Padovani P., Matteucci F., 1993, *ApJ*, 416, 26
- Papadopoulos P. P., 2010, *ApJ*, 720, 226
- Papadopoulos P. P., Thi W.-F., Miniati F., Viti S., 2011, *MNRAS*, 414, 1705
- Peebles M. S., Werk J. K., Tumlinson J., Oppenheimer B. D., Prochaska J. X., Katz N., Weinberg D. H., 2014, *ApJ*, 786, 54
- Pflamm-Altenburg J., Weidner C., Kroupa P., 2007, *ApJ*, 671, 1550
- Pipino A., Devriendt J. E. G., Thomas D., Silk J., Kaviraj S., 2009, *A&A*, 505, 1075
- Pipino A., Matteucci F., 2004, *MNRAS*, 347, 968
- Planck Collaboration XVI 2014, *A&A*, 571, A16
- Popping G., Caputi K. I., Trager S. C., Somerville R. S., Dekel A., Kassim S. A., Kocevski D. D., Koekemoer A. M., Faber S. M., Ferguson H. C., Galametz A., Grogin N. A., Guo Y., Lu Y., Wel A. v. d., Weiner B. J., 2015, *MNRAS*, 454, 2258
- Pozzetti L., Cimatti A., Zamorani G., Daddi E., Menci N., Fontana A., Renzini A., Mignoli M., Poli F., Saracco P., Broadhurst T., Cristiani S., D’Odorico S., Giallongo E., Gilmozzi R., 2003, *A&A*, 402, 837
- Recchi S., Calura F., Kroupa P., 2009, *A&A*, 499, 711
- Salpeter E. E., 1955, *ApJ*, 121, 161
- Sánchez S. F., Kennicutt R. C., Gil de Paz A., van de Ven G., Vílchez J. M., Wisotzki L., Walcher C. J., Mast D., et al. 2012, *A&A*, 538, A8
- Saracco P., Fiano A., Chincarini G., Vanzella E., Longhetti M., Cristiani S., Fontana A., Giallongo E., Nonino M., 2006, *MNRAS*, 367, 349
- Segers M. C., Schaye J., Bower R. G., Crain R. A., Schaller M., Theuns T., 2016, *MNRAS*, 461, L102
- Smith R. J., 2014, *MNRAS*, 443, L69
- Smith R. J., Lucey J. R., Conroy C., 2015, *MNRAS*, 449, 3441
- Spolaor M., Kobayashi C., Forbes D. A., Couch W. J., Hau G. K. T., 2010, *MNRAS*, 408, 272
- Springel V., White S. D. M., Jenkins A., Frenk C. S., Yoshida N., Gao L., Navarro J., Thacker R., Croton D., Helly J., Peacock

- J. A., Cole S., Thomas P., Couchman H., Evrard A., Colberg J., Pearce F., 2005, *Nature*, 435, 629
- Tacconi L. J., Genzel R., Neri R., Cox P., Cooper M. C., Shapiro K., Bolatto A., Bouché N., et al. 2010, *Nature*, 463, 781
- Tacconi L. J., Neri R., Genzel R., Combes F., Bolatto A., Cooper M. C., Wuyts S., Bournaud F. e. a., 2013, *ApJ*, 768, 74
- Thielemann F.-K., Argast D., Brachwitz F., Hix W. R., Höflich P., Liebendörfer M., Martinez-Pinedo G., Mezzacappa A., Nomoto K., Panov I., 2003, in Hillebrandt W., Leibundgut B., eds, *From Twilight to Highlight: The Physics of Supernovae Supernova Nucleosynthesis and Galactic Evolution*. Springer-Verlag, Berlin, p. 311
- Thomas D., Maraston C., Bender R., Mendes de Oliveira C., 2005, *ApJ*, 621, 673
- Thomas D., Maraston C., Johansson J., 2011, *MNRAS*, 412, 2183
- Thomas D., Maraston C., Schawinski K., Sarzi M., Silk J., 2010, *MNRAS*, 404, 1775
- Trager S. C., Faber S. M., Dressler A., 2008, *MNRAS*, 386, 715
- Trager S. C., Faber S. M., Worthey G., González J. J., 2000, *AJ*, 119, 1645
- Tremonti C. A., Heckman T. M., Kauffmann G., Brinchmann J., Charlot S., White S. D. M., Seibert M., Peng E. W., Schlegel D. J., Uomoto A., Fukugita M., Brinkmann J., 2004, *ApJ*, 613, 898
- Walcher C. J., Wisotzki L., Bekeraité S., Husemann B., Iglesias-Páramo J., Backsmann N., Barrera Ballesteros J., Catalán-Torrecilla C., et al. 2014, *A&A*, 569, A1
- Wang J., De Lucia G., Kitzbichler M. G., White S. D. M., 2008, *MNRAS*, 384, 1301
- Weidner C., Kroupa P., 2005, *ApJ*, 625, 754
- Weidner C., Kroupa P., Larsen S. S., 2004, *MNRAS*, 350, 1503
- Weidner C., Kroupa P., Pflamm-Altenburg J., 2011, *MNRAS*, 412, 979
- Weidner C., Kroupa P., Pflamm-Altenburg J., Vazdekis A., 2013, *MNRAS*, 436, 3309
- Yates R. M., Henriques B., Thomas P. A., Kauffmann G., Johansson J., White S. D. M., 2013, *MNRAS*, 435, 3500
- Zibetti S., Charlot S., Rix H., 2009, *MNRAS*, 400, 1181